JOURNAL OF MATERIALS SCIENCE 20 (1985) 491–500

Microstructural damage due to dynamic loading of Cu–Co dispersion alloys

K. V. RAO*, D. H. POLONIS
Department of Materials Science and Engineering, University of Washington, Seattle, WA 98195, USA

Transmission electron microscopy techniques have been employed to study the microstructural changes accompanying deformation and spallation during the dynamic loading of Cu–Co dispersion alloys. Alloys aged to produce coherent precipitate particles exhibited a loss of coherency and apparent precipitate enlargement after being subjected to dynamic loading conditions. Over-aged alloys containing incoherent precipitates exhibited precipitate growth, dislocation entanglements and void initiation in the matrix adjacent to precipitate–matrix interfaces. The superior spallation resistance of alloys containing fine coherent precipitates is attributed to the difficulty of void nucleation at low misfit interfaces which can accommodate dislocation cutting and offer preferred sinks for excess vacancies. A model based on the generation of excess lattice vacancies during dynamic loading is described to account for the observation of particle enlargement and loss of coherency, as well as the preferred initiation of voids adjacent to incoherent particles.

1. Introduction

The microstructural damage produced in alloys during dynamic loading and the resistance to spallation fracture are sensitive to the presence of impurity second phase particles [1, 2]; the coherent or incoherent nature of the precipitate–matrix interface associated with precipitate particles is another important consideration [3]. It has been suggested that porosity or void formation can be inhibited and spallation resistance can be improved by employing fine dispersions of coherent precipitate particles; however, limited previous investigations have been reported concerning the influence of fine coherent dispersions on the deformation and fracture behaviour for dynamic loading conditions. Dense arrays of fine thoria particles in TD nickel and TD nickel–chrome alloys have been shown to prevent the formation of twins or dislocation cell structures [4]. It was reported [5] that coherent precipitates in Inconel 600 exhibit a loss of coherency at dynamic pressures above 200 kbar; similar observations have been made in precipitation hardened aluminium alloys [6]. The present paper reports on the influence of coherent and incoherent precipitates on the microstructural damage and the processes of fracture initiation in a precipitation alloy subjected to varying ageing treatments.

Copper–cobalt alloys were selected as the model system for this investigation since they can be treated to produce random dispersions of either coherent or incoherent precipitate particles with spherical morphologies. The low misfit strain in this system also makes it possible to produce a wide range of precipitate sizes with coherency maintained up to approximately 70 nm diameter [7]. This ability to produce a variety of dispersion conditions provides an opportunity to examine the influence of particle size and coherency on the initiation of ductile fracture in two-phase alloys.

2. Experimental procedures

Cu–Co alloys containing 1.95% and 2.8% cobalt† were prepared from OFHC copper and electrolytic

*Present address: Cabot Wrought Products Division, Cabot Corp., 1020 W. Park Avenue, Kokomo, IN 46901, USA.
†Compositions are given in wt %.

0022–2461/85 $03.00 + .12

grade cobalt by vacuum induction melting in a graphite crucible. The alloys were cast in the form of 2 cm diameter rods; the alloy rods were homogenized at 100° C for 24 h, followed by cold swaging in step reductions to 13 cm diameter, with intermediate annealing at 650° C. Hollow cylindrical test specimens 5 mm i.d., 10 mm o.d. and 19.1 mm long were machined from the rods for the dynamic loading experiments. These hollow test cylinders were solution treated at 965° C for 2 h, followed by rapid quenching in iced brine; the solution-treated and quenched Cu–Co alloys were then aged at 650° C. Prior to all heat-treatments the specimens were sealed in vycor or quartz capsules which were evacuated and back-filled with a partial pressure of purified argon.

An exploding wire system developed by Fyfe [8] was employed to generate biaxial strain dynamic loading conditions in the hollow cylindrical specimens. Dynamic loading is achieved by discharging stored energy (6000 to 9000 J) through a 1.84 mm diameter copper wire enclosed in a polyethylene jacket, 5.03 mm in diameter. The discharge causes a very rapid vaporization of the copper wire which drives the polyethylene jacket radially outward until it impacts with the inner surface of the hollow cylinder. The system generates a pressure pulse having a rise time of approximately 0.1 μsec with a maximum load as high as 25 kbar. Depending on the loading condition and specimen dimensions, varying levels of damage result, ranging from random void generation to incipient or complete spallation. The magnitude of the peak tensile stress associated with the reflected stress wave determines whether or not spallation occurs. Complete spallation is characterized by a well defined, continuous internal fracture surface concentric with the cylindrical surfaces of the specimen. The response of an individual specimen is determined by the specimen geometry, the microstructure of the materials and the magnitude of the stress pulse.

Thin foil specimens for transmission electron microscopy (TEM) work were prepared from material removed from different radial positions between the internal impact surface and the outer surface of the dynamically loaded samples. Thin disc specimens were electropolished in a jet polisher using a solution containing two parts of orthophosphoric acid and one part of distilled water at 50 to 70 V. During the thinning process efforts were made to produce perforations close to the centre of each foil in order to assist in locating the approximate position of the microstructure with respect to the impact surface. The thin foils were examined by transmission in a Phillips EM-300 electron microscope operated at 100 kV.

3. Experimental results

Table I lists the schedule of heat treatments and the corresponding microstructures for the 1.9% and 2.8% cobalt alloys subjected to dynamic loading in the present investigation. The treatments were designed to compare the effects of standardized dynamic loading conditions on alloys in the solution-treated, peak-aged and over-aged conditions. The response to dynamic loading was sensitive to the heat treatment for both compositions. When subjected to identical loading conditions the specimens of both alloys aged to peak strength showed less spall damage in comparison with the solution-treated or over-aged conditions. The over-aged specimens suffered the most extensive fracture damage, as evidenced by well-defined internal fracture patterns, including radial cracking and spallation. The occurrence of a well-defined spall plane in the solution-treated alloys and incipient spall [3] in the over-aged specimens can be seen in Fig. 1. While the two compositions exhibited generally similar behaviour, the Cu–2.8% Co specimens displayed higher resistance to internal spall cracking when compared to the comparably treated 1.95% Co alloy specimens. In general, the Cu–2.8% Co alloy aged to the peak strength condition displayed maximum resistance to spallation damage. The over-aged specimens exhibited the maximum degree of overall damage with respect to the propensity toward radial crack formation.

TEM examination of the alloys prior to

TABLE I Heat treatments

Alloy composition	Heat treatment	Microstructure
Cu–1.95% Co	SHT 965° C/2 h	single phase α
Cu–1.95% Co	SHT, peak-aged 650° C/180 min	α + coherent particles
Cu–1.95% Co	SHT, over-aged 650° C/10 days	α + incoherent precipitates
Cu–2.8% Co	SHT, 965° C/2 h	single phase α
Cu–2.8% Co	SHT, peak-aged 650° C/150 min	α + coherent particles
Cu–2.8%	SHT, over-aged 650° C/8 days	α + coherent precipitates

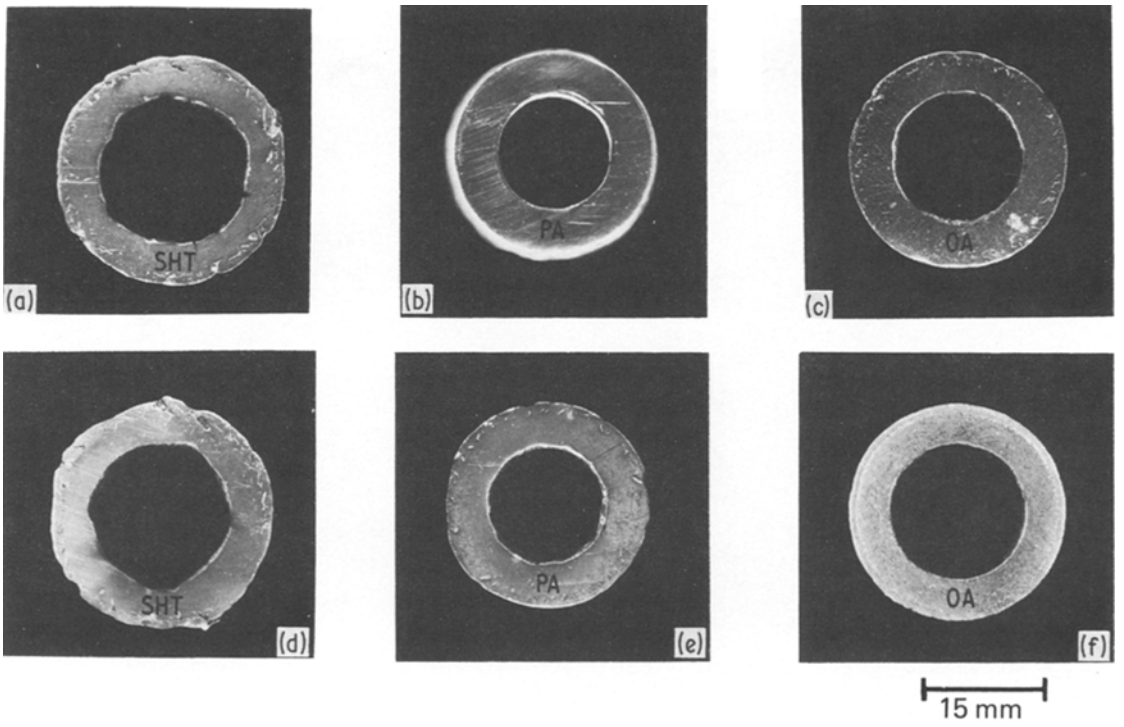

Figure 1 Macrographs showing the influence of ageing on the damage resulting from identical dynamic loading conditions, (a)–(c): Cu–1.95% Co; and (d)–(f): Cu–2.8% Co alloys. (SHT = solution-heat treated, PA = peak-aged, OA = over-aged.)

dynamic loading confirmed that single phase microstructures were always obtained in the solution-treated condition. Fine coherent precipitates were observed in both alloys heat-treated to the peak strength condition; the strain contrast associated with the typical spherical particles is illustrated in Fig. 2 for the Cu–2.8% Co alloy aged 150 min at 650° C. The cobalt-rich precipitates were characterized in the microstructure by the appearance of the line of no contrast flanked by two dark symmetrical lobes. Average particle diameters of 16 ± 2 nm were determined from the micrographs taken from the peak-aged alloys. The appearance of the precipitate particles in Fig. 2 and the corresponding particle sizes are in agreement with results reported previously [9] for Cu–Co alloys of similar compositions subjected to similar heat treatments. The over-aged alloy specimens exhibited incoherent cobalt-rich precipitates having average diameters of 70 ± 5 nm.

The dynamically loaded solution-treated alloy specimens exhibited high densities of dislocations in the form of tangles and cell structures, as shown in Fig. 3 for a 2.8% Co alloy. The long straight dislocations forming the cell boundaries in this figure were also characteristic features of the Cu–1.95% Co alloy after dynamic deformation. These dislocation configurations are similar to the structures reported in shock-loaded copper [10], and in dilute copper alloys, such as Cu–0.67% Si [11] and Cu–1.1% Al [12] alloys. The cells observed in the dynamically loaded Cu–Co alloys exhibited fairly uniform sizes ranging from 0.1 to 0.15 μm.

The predominant microstructural feature of the dynamically deformed peak-aged alloys was the apparent loss of coherency of the initially coherent precipitates; this was manifested by the absence of the line of no contrast, and the appearance of misfit dislocations at the precipitate interfaces, as shown in Fig. 4a for the 1.95% Co alloy. A representative microstructure from a region close to the impact surface of the Cu–2.8% Co alloy is shown in Fig. 4b. Figs. 4a and b indicate that not all of the precipitates have lost coherency, but the density of incoherent particles increases with increasing distance from the impact surface. In regions near the potential spall plane large numbers of particles exhibited a loss of coherency; a typical example of the microstructure in this region is shown in Fig. 5a for the 2.8% Co alloy.

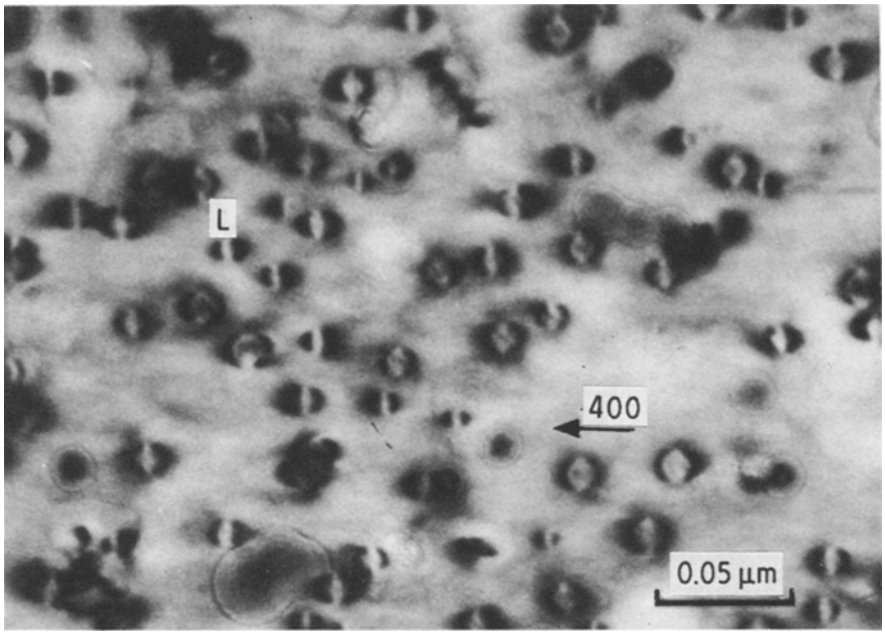

Figure 2 Transmission electron micrograph of Cu–2.8% Co alloy aged at 650° C for 150 min, showing coherent precipitates with bands of no contrast marked L. Operating reflection (400).

The coherency loss observed in a thin foil obtained from a region close to the outer edge of the cylindrical specimen is shown in Fig. 5b.

The microstructures of the peak-aged alloys subjected to dynamic loading showed an apparent increase in the size of the precipitates. The precipitate size measured between the impact surface and the outer radius varied from 18 to 35 nm in diameter. Some precipitates, such as those marked in Fig. 4a and b, were still coherent in regions close to the impact surface. However, precipitate diameters of 30 ± 5 nm were consistently observed in regions adjacent to the potential spall plane, as illustrated in Figs. 5a and b. Such increased precipitate sizes following dynamic loading agree with the particle growth reported in under-aged Al–4.65% Cu alloys subjected to shock loading [6].

The over-aged alloys which contained incoherent precipitates after solution treatment and ageing exhibited a high density of micro-voids as a

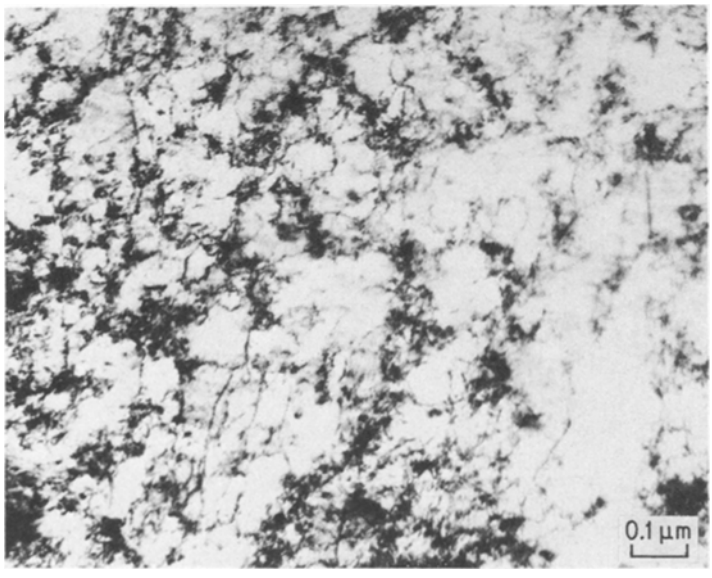

Figure 3 Transmission electron micrograph showing dislocation tangles and cell structures formed during dynamic loading in the solution-treated Cu–2.8% Co alloy.

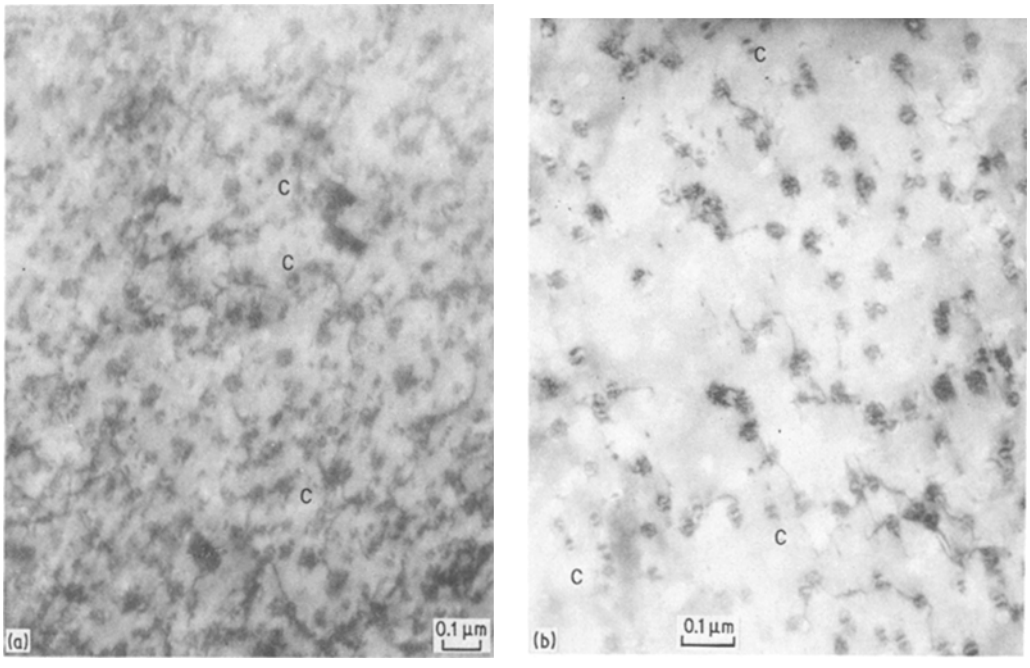

Figure 4 Transmission electron micrographs of alloys peak-aged and subjected to dynamic loading. (a) Cu–1.95% Co alloy aged for 180 min at 650° C showing loss of coherency of the pre-existing coherent precipitates and the presence of misfit dislocations. Some precipitates, marked C, still retain coherency after deformation. (b) Cu–2.8% Co alloy aged for 150 min at 560° C showing coherency loss and increase in precipitate size ~ 0.4 mm from the impact surface. Some precipitates, shown at C, are still coherent.

result of dynamic loading. Void development was evident along the interfaces separating the cobalt-rich precipitates and the copper matrix. Typical micro-void observations are shown in Fig. 6a where they appear as white regions in the vicinity of the precipitate-matrix interfaces, as shown at points marked A. Micro-voids were also observed along the grain boundaries and especially at boundary precipitate sites in the dynamically loaded over-aged alloys, as shown at X in Fig. 6b. The voids identified in Figs. 6a and b are similar to those accompanying decohesion at η-phase

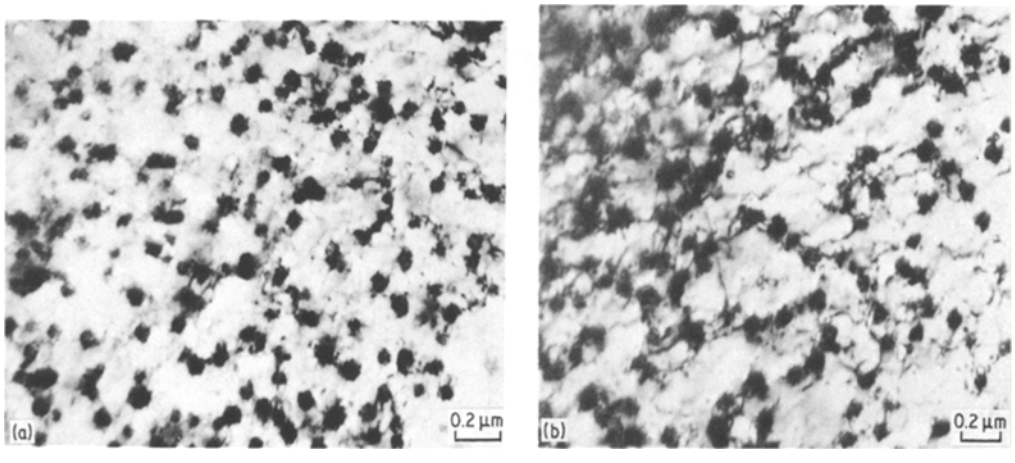

Figure 5 Transmission electron micrographs taken from regions near the potential spall plane of dynamically loaded Cu–2.8% Co alloy cylinders aged at 650° C for 150 min. (a) Coherency loss and precipitate enlargement. (b) Loss of coherency and a higher dislocation density compared to Fig. 4b in a region between the spall plane and the outer surface.

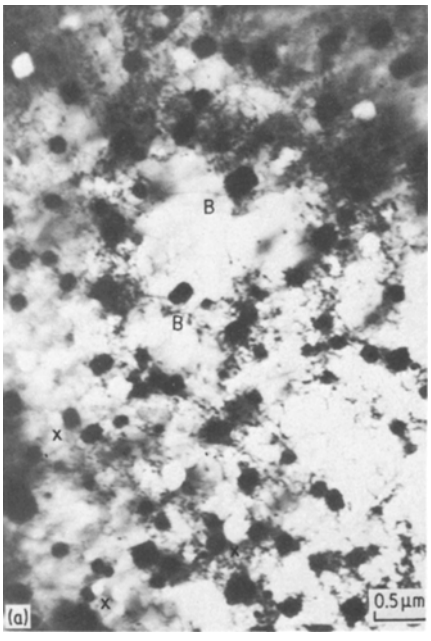

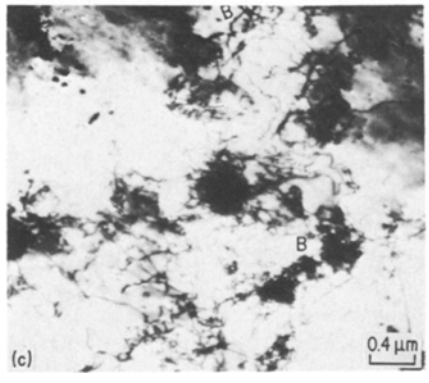

Figure 6 Transmission electron micrographs obtained from regions near the potential spall plane of dynamically loaded Cu–2.8% Co alloy cylinders aged at 650° C for 8 days. (a) Shows large precipitates and void formation marked X in close proximity to incoherent particles. (b) Shows voids at precipitate particles marked X and along a grain boundary interface. (c) Shows heavy dislocation structure and evidence for bending at B.

precipitates in irradiated 316 stainless steel [13]. The over-aged alloys also exhibited apparent precipitate enlargement over the entire thickness of the specimen as a result of dynamic loading. The precipitate diameters increased from approximately 70 nm in the undeformed condition to a maximum of 350 nm in the spall fracture zone after dynamic loading. Accurate determinations of the precipitate sizes were not possible due to the dense dislocation tangles around the precipitates as shown in Fig. 6c. However, the increases in precipitate size illustrated in Figs. 6a to c are in agreement with the particle growth reported to occur in over-aged Al–4.65% Cu deformed by shock loading [6].

4. Discussion of results

4.1. General microstructural damage

The dense dislocation tangles and diffuse dislocation cell structures produced by dynamic loading in the solution-treated Cu–Co alloys are generally similar to those observed in pure copper and other dilute copper-based alloys. The cell sizes of 0.1 to 0.15 μm determined in the present work resulted from dynamic loading to 18 to 20 kbar pressure at the inner loading boundary [8]. On the other hand, cell sizes approximating 0.3 μm were reported in copper after deformation by plane shock waves at 90 kbar [10]. Vora *et al.* [11], showed that the large tensile hoop stress produced by biaxial dynamic loading of hollow cylinders results in severe plastic deformation in local regions of the specimen. It was also shown that even at low loading levels the cylindrical specimens are subjected to larger plastic strains than the same material subjected to plane shock wave loading at much higher shock pressures. The smaller cell size obtained in the present study is indicative of heavy plastic deformation [14] and is consistent with the expectation of severe plastic strain at relatively low pressures under biaxial strain conditions.

The present investigation revealed or confirmed several important phenomena with respect to the response of dispersion alloys to dynamic loading. Several differences between dynamic and quasi-static loading conditions are also noted.

1. In alloys aged to peak strength the cobalt-rich precipitates tend to lose coherency with the matrix as a result of dynamic loading. This was especially evident near the potential spall surface

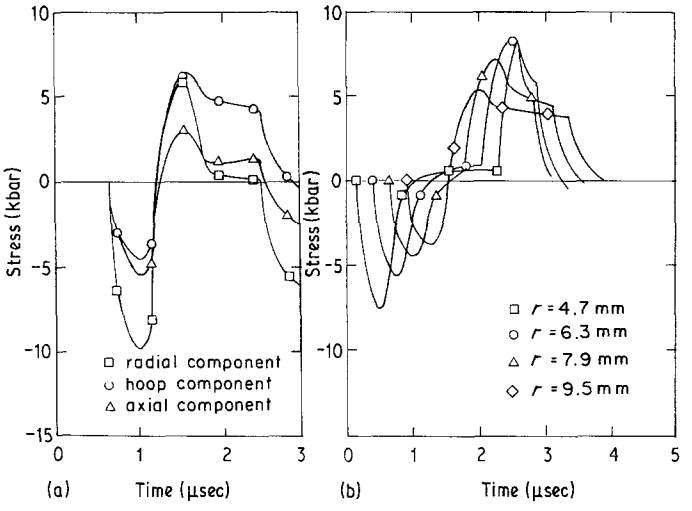

Figure 7 Typical stress histories for hollow cylindrical specimens subjected to dynamic loading under biaxial conditions (determined for 6061-T651 Al alloy). (a) Stress history at the spall plane [16]. (b) Hoop stress history at four radii [16].

where the greatest fraction of precipitate particles exhibited coherency loss, as shown in Figs. 4a, 4b and 5a. After quasi-static deformation the majority of the precipitate particles in peak-aged alloys retained coherency; there was a high density of dislocation dipoles but extra dislocations were not observed at the precipitate interfaces.

2. Definite precipitate particle growth was observed for both peak-aged and over-aged alloys subjected to plastic deformation at high strain rates. The particle diameters increased from an average of 16 to 35 nm in the peak-aged condition and from 75 to 350 nm in the over-aged condition; this observation is consistent with the precipitate growth reported in dynamically loaded Al–4.65% Cu alloys [6].

3. Dense dislocation tangles were evident around the incoherent particles as a result of dynamic loading. The density of these tangles contributed to the difficulty of determining accurate precipitate particle sizes after dynamic loading.

4. Numerous micro-voids were observed at precipitate–matrix interface sites and along the grain boundaries in the over-aged alloys after static and dynamic loading, but were not evident in alloys aged to peak strength. In addition to the coherency loss in the peak strength alloys the microstructures in the vicinity of the spall surface exhibited "dark spots" similar to those identified with vacancy clusters and defects introduced by radiation damage in other metals [15].

4.2. Precipitate growth due to dynamic loading

The dispersion alloys in both the peak-aged and over-aged conditions exhibited dramatic precipitate particle growth as a result of dynamic loading, as shown in Figs. 4a, 5b, 6a and 6b. The definite increase in the number of precipitates losing coherency with increasing distance from the loading boundary can be attributed to the large stress gradients that exist across the wall thickness of the cylinder [16]. The stress distributions calculated for cylindrical aluminium alloy specimens using a materials constitutive equation and the inner boundary loading history are shown in Fig. 7 [16]. These particular stress histories refer to 6061-T6 aluminium alloys, but the relative relationships are independent of the metal used [3]. The important effect to note from Fig. 7 is the variation of each of the principal stresses as a function of radius in a manner which is unique to the cylindrical geometry. Such variations in stress result in non-homogeneous deformation along the radial directions, thereby accounting for the difference in the number of particles exhibiting a loss of coherency across the wall thickness.

The precipitate particles in the peak-aged alloys were enlarged by a factor of two and those in the over-aged condition by a factor of four. This increase in precipitate size marked the principal difference between the deformed structures resulting from dynamic loading conditions when compared to quasi-static loading. The dramatic change in microstructure can be explained in terms of excess vacancies generated during dynamic loading. Although only indirect evidence for the production of such vacancies has been obtained in the present work, the microstructural observations are

TABLE II Production of vacancies during dynamic loading

Authors	Material	Comments
Weertman [17]	Theoretical	Predicted on the basis of dislocation theory that rapid loading induces vacancy supersaturation.
Kressel *et al.* [18]	Ni	Electrical resistivity measurements showed that high concentrations of point defects are created in shock-loaded Ni, and that they are predominantly vacancies.
Murr *et al.* [19]	304 stainless steel	Showed that whereas at 425 kbar the volume fraction of twinned material is about 43%, the residual hardness of 304 stainless steel shock loaded at 750 kbar is about 10% greater than at 425 kbar and the corresponding twin volume density is only 10%. It was suggested that the only possible explanation for this feature is a significant strengthening due to point defects – presumably vacancies.
Murr *et al.* [4]	Ni, TD–Ni, Chromel-A Inconel 600 and TD–NiCr	The dramatic thermal recovery of the shocked hardness of Ni samples subjected to pressures above 750 kbar was attributed to the presence of appreciable concentrations of vacancies.
Murr *et al.* [20]	Inconel 600	Thermal recovery of shock-loaded and explosively formed Inconel 600 was characterized by an absence of recrystallization. This was explained on the basis of a mechanism which involves the formation of large numbers of vacancies or vacancy clusters.
Greenhut *et al.* [6]	Al–4.6% Cu	The production of excess vacancies during high strain rate loading has been shown to depend on the net tension resulting from the interaction of the reflected tensile wave and the unloading portion of the compressive wave. It was suggested that the large numbers of excess vacancies contribute to precipitate growth.

consistent with the conclusions of previous workers summarized in Table II relevant to the generation of vacancies during high strain rate deformation. The present experimental conditions are compatible with the requirements set forth for the production of excess vacancies. The high intensity net tensile stress resulting from the interaction of the reflected tensile wave and the unloading portion of the compressive wave, as shown in Fig. 7, facilitates the production of excess vacancies with the maximum concentration expected in the vicinity of the potential spall plane where the net tensile stress reaches a maximum value. Furthermore, regions close to the impact surface where the compressive wave amplitude predominates are expected to yield relatively few excess vacancies, since it has been shown that net tension provides favourable conditions for vacancy generation while compression does not [6, 21]. This qualitative argument is consistent with the microstructural observations indicating that coherency loss and precipitate enlargement are associated directly with the magnitude of the tensile component of the stress wave.

The precipitate enlargement resulting from plastic deformation under dynamic loading conditions is therefore interpreted as the result of enhanced diffusion resulting from the combined effects of intense local heating in the material and a vacancy supersaturation. Rapid loading conditions such as those employed in this investigation are expected to result in severe local heating due to adiabatic compression. This explanation is supported by the conclusions of previous workers for other systems [4, 5]. The shock hardening in 304 stainless steel and the thermal recovery of Inconel 600 were accounted for in terms of excess vacancies generated during dynamic loading. In another investigation [18] electrical resistivity measurements were used to show that high concentrations of point defects, predominantly vacancies, are created in shock-loaded nickel.

The diffusional growth of incoherent cobalt-rich precipitates is difficult to explain since the process must involve a "ripening" or coarsening mechanism. The precipitate particle growth in such cases requires solute transport to the larger particles by means of a vacancy dependent

mechanism [22]. The generation of excess vacancies under dynamic conditions is apparently sufficient in the case of copper–cobalt alloys to provide the necessary diffusion rates for observable particle growth. A precedent for this type of reaction has been reported in Al–4.65% Cu alloys subjected to shock deformation [6] and in several other aluminium alloys that exhibited the vacancy-assisted growth of grain boundary precipitates adjacent to "denuded" or precipitate-free zones [23]. These earlier findings are consistent with the observations in the current study where particle growth is a maximum in regions adjacent to the potential spall plane where the net tensile pulse reaches a maximum intensity.

4.3. Void formation and fracture initiation

Uniform dispersions of fine precipitates have been suggested as a likely means of controlling void formation that might result from vacancy condensation in irradiated metals [15]. This behaviour is reflected in the microstructures of the current study where the peak-aged alloys exhibited precipitate enlargement without the formation of interfacial voids. The observations support the notion that coherent precipitates can offer effective sinks for excess vacancies created during dynamic loading.

The present results show that precipitates which are nearly 20 nm in diameter remain coherent after dynamic deformation as shown at points marked C in Figs. 4a and b, whereas particles in the range 20 to 35 nm diameter tend to lose coherency during loading, as illustrated in Figs. 4 and 5. These observations agree with Amin *et al.* [24], who predicted on the basis of an argument by Brown and Ham [25] that particle diameters approximating 22 nm correspond to a critical size below which coherency is retained after deformation. The experimental observations of Amin *et al.* indicated a critical particle diameter of about 30 nm for inducing coherency loss during standard tensile testing of Cu–Co alloys.

Since many of the coherent particles are sheared by dislocations during dynamic loading the conditions in the vicinity of the coherent particles differ considerably from those for incoherent particles where dislocation tangles are expected to develop. In both cases vacancy-enhanced diffusion of solute to the precipitate particles is expected to occur, but the intense dislocation tangles in the vicinity of incoherent particles will be more conducive to the generation of voids since heterogeneous sites for void nucleation exist and vacancy accumulation resulting from dislocation interactions can occur. The pile-ups generate vacancies that are in close proximity to the interfaces offering preferred sites for void nucleation. In the case of coherent particles, dislocations shear the particles and fewer lattice vacancies develop because of fewer dislocation interactions. Consequently, conditions favouring the development and migration of lattice vacancies exist where a high dislocation density develops due to entanglements in the vicinity of incoherent particles. This is also reflected by the fact that the apparent growth exhibited by the incoherent particles is considerably greater than that for the coherent particles.

The initiation of spallation fracture has been identified with micro-crack or void initiation at existing flaws or inhomogeneities subjected to high stress levels during deformation [1]. In high purity metals and single phase alloys where second phase particles are absent, micro-voids can nucleate at grain boundaries, dislocation configurations or in the matrix itself [26, 27]. The superior spallation resistance of the peak-aged Cu–Co alloys can be understood in terms of the difficulty of nucleating voids at coherent interfaces. On the other hand, particles that undergo sufficient growth to develop incoherency during dynamic loading and those that are incoherent in the initial aged condition offer preferred sites for void initiation due to vacancy condensation or interfacial decohesion at incoherent interfaces. The superior spallation resistance of peak-aged alloys in the present work agrees with previous work on Al alloys [28, 29] that showed higher spallation resistance in the under-aged condition as compared to over-aged alloys. The formation of microscopically resolvable voids in Cu–Co alloys, in conjunction with particles approximately 100 nm in diameter, confirms the susceptibility of alloys to spallation damage when incoherent particles promote dislocation pile-ups and tangles, as opposed to particle shear in the case of coherent particles.

5. Conclusions

1. Cu–Co alloys aged to the peak hardened condition exhibit superior resistance to spallation damage in comparison with similar compositions in the solution-treated or over-aged conditions.

2. The experimental results indicate that plastic deformation under dynamic conditions leads to coherency loss of pre-existing coherent particles; precipitate particle enlargement and the formation of voids at incoherent precipitate–matrix interfaces and grain boundaries also occurs. The magnitude of these effects is a maximum near the potential spall surface corresponding to the position of the highest net tensile stress during the dynamic loading of hollow cylinders.

3. On the basis of the microstructural evidence it is concluded that excess lattice vacancies generated during dynamic loading account in part for precipitate growth and the nucleation of microvoids. It is also expected that the process of particle growth contributes to the coherency loss experienced by larger particles in the peak-aged alloys.

4. The superior spallation resistance of the peak-aged alloys is attributed to the relaxation of elastic strains around coherent precipitates by dislocation cutting rather than the formation of tangles and to the effectiveness of coherent precipitates as preferred sinks for excess vacancies. Dense dislocation entanglements in the matrix surround the incoherent particles after dynamic loading, providing favourable conditions for vacancy migration and clustering in the vicinity of the interfaces.

Acknowledgements

The authors acknowledge with thanks the assistance of the US Bureau of Mines, Albany, Oregon in the preparation of Cu–Co alloy ingots used in the present study. Special thanks are expressed to Professor I. M. Fyfe for his valuable discussions and for making his dynamic test facility available for this study.

References

1. D. A. SHOCKEY, L. SEAMAN and D. R. CURRAN, in "Metallurgical Effects at High Strain Rates", edited by R. W. Rohde, B. M. Butcher, J. R. Holland and C. H. Karnes (Plenum, New York, 1973) p. 473.
2. S. E. AXTER, W. B. JONES and D. H. POLONIS, *Metallography* 8 (1975) 425.
3. W. B. JONES and H. I. DAWSON, in "Metallurgical Effects at High Strain Rates", edited by R. W. Rohde, B. M. Butcher, J. R. Holland and C. H. Karnes (Plenum, New York, 1973) p. 443.
4. L. E. MURR and H. R. VYDYANATH, *Scripta Metall.* 4 (1970) 183.
5. L. E. MURR and J. V. FOLTZ, *J. Appl. Phys.* 40 (1969) 3796.
6. V. A. GREENHUT, M. G. CHEN, R. BENCK and S. K. GOLASKI, Proceedings of the 2nd International Conference on Mechanical Behavior of Materials, Boston (American Society for Metals, Ohio, 1976) p. 1790.
7. J. D. LIVINGSTON, *Trans. Met. Soc. AIME* 215 (1959) 566.
8. I. M. FYFE and R. R. ENSMINGER, *J. Mech. Phys. Solids* 14 (1966) 231.
9. V. A. PHILLIPS and J. D. LIVINGSTON, *Phil. Mag.* 7 (1962) 969.
10. J. GEORGE, *ibid.* 15 (1967) 497.
11. H. VORA, I. M. FYFE and D. H. POLONIS, *Mater. Sci. Eng.* 32 (1978) 129.
12. O. JOHARI and G. THOMAS, *Acta Metall.* 12 (1964) 1153.
13. L. K. MANSUR, M. R. HAYNS and E. H. LEE, Materials Science Program, Oak Ridge National Labs., TM-7970, June (1981) p. 177.
14. Y. KOMEM and J. REZEK, *Met. Trans.* 6A (1975) 549.
15. D. I. R. NORRIS, *Rad. Effects* 14 (1972) 1.
16. I. M. FYFE and R. M. SCHMIDT, University of Washington, Dept. of Aero. and Astro., Report 72-10 (1972).
17. J. WEERTMAN, in "Response of Metals to High Velocity Deformation", edited by P. G. Shewmon and V. F. Zackay (Interscience, New York, 1961) p. 205.
18. H. KRESSEL and N. BROWN, *J. Appl. Phys.* 38 (1967) 1618.
19. L. E. MURR, J. V. FOLTZ and F. D. ALTMAN, *Phil. Mag.* 23 (1971) 1011.
20. L. E. MURR and B. H. MADDALA, *Mater. Sci. Eng.* 7 (1971) 286.
21. R. W. BALLUFFI and L. L. SEIGLE, *Acta Metall.* 3 (1955) 170.
22. A. KELLY and R. B. NICHOLSON, *Prog. Mater. Sci.* 10 (1963) 3.
23. E. A. STARKE Jr, *J. Metals.* Jan. (1970) 546.
24. K. E. AMIN, V. GEROLD and G. KRALIK, *J. Mater. Sci.* 10 (1975) 1519.
25. L. M. BROWN and R. K. HAM, in "Strengthening Methods in Crystals", edited by A. Kelly and R. B. Nicholson (Elsevier, Amsterdam, 1971) p. 53.
26. A. L. STEVENS, L. DAVISON and W. E. WARREN, *J. Appl. Phys.* 43 (1972) 4922.
27. R. PAGE and J. R. WEERTMAN, *Scripta Metall.* 14 (1980) 1029.
28. A. M. DIETRICH, V. A. GREENHUT and S. GOLASKI, Proceedings of US Army Science Conference (1974) p. 247.
29. R. B. HERRING and G. B. OLSON, AMMRC, Watertown, Mass., TR 71-61, Dec. (1971).

Received 6 March
and accepted 27 March 1984